Role of radius on prewetting behavior in nematic liquid-crystal droplets

Erfan Kadivar*
Department of Physics, Faculty of Sciences, Persian Gulf University, 75168 Bushehr, Iran
(Received 21 April 2009; published 1 July 2009)

The prewetting phenomena in a nematic liquid crystal confined to a droplet embedded in a spherical solid surface are discussed. This paper is based on Landau–de Gennes theory and Nobili-Durand surface energy. By using a Maxwell construction, we find that the first-order boundary-layer transition inside of droplet which vanishes completely below a critical radius R_c when bulk nematic isotropic transition temperature is approached from above. We obtain a narrow temperature interval above the bulk nematic-isotropic phase transition which corresponds to nematic boundary layer inside of droplet. The interval length depends on surface potential and droplet radius. We also find that there is no critical radius for boundary transition when the nematic-isotropic transition temperature is approached from below.

DOI: 10.1103/PhysRevE.80.011701 PACS number(s): 61.30.Hn, 61.30.Pq, 61.30.Cz

I. INTRODUCTION

During the last few years, much attention has been paid to the geometry of surface in a liquid crystal since interesting phenomena arise through the combination of liquid crystal and surface geometry. The surface phenomena in the nematic liquid crystal were first studied by Sheng, which he called boundary-layer transition [1]. Most theoretical studies of such transitions have been confined to planar substrate [1–5].

Both the density-functional theory and the Landau–de Gennes theory lead to the result that the surface phase diagram is severely restricted as a result of the nonplanar geometry. Using the Landau–de Gennes theory, wetting on other geometries such as cylinder and spherical which are dispersed in the nematic liquid crystal has been studied [6–9]. The possible phases in a nematic liquid crystal confined to a spherical droplet were analyzed in term of Landau–de Gennes theory [10]. The density-function theory has also been used to study the wetting behavior at hard spheres, cylinders, and ellipsoids [11–15].

The wetting behavior in nematic liquid-crystal droplet depends on surface anchoring (orientation of the liquid-crystal director at an interface). The radial, axial, bipolar, twisted bipolar, and concentric configurations are observed in the nematic droplet. The radial and axial anchoring states relate to the homeotropic anchoring, and other configurations correspond to the planar anchoring. The director field configuration of a nematic liquid crystal confined to a spherical cavity within a urethane polymer is observed to transform from a radial to axial configuration as function of radius of cavity, temperature, anchoring strength, and external electric field [16].

In this work, the role of curvature on nematic wetting is investigated in the nematic droplet. This work is based on Landau–de Gennes theory and quadratic surface energy. We obtain a phase diagram which presents the wetting behavior as function of surface potential.

II. LANDAU–GINZBURG–DE GENNES THEORY

Consider a spherical droplet which is located at origin. We want to study the role of curvature on wetting layer both for below nematic-isotropic temperature but also for above nematic-isotropic temperature. To study the wetting phenomena, we start with the Landau–de Gennes theory. This theory is based on second-rank tensor and traceless tensor $Q_{ij}(\mathbf{r})$ which is also called the alignment tensor [17]. The eigenvectors of Q_{ij} represent the axes of main molecular orientation, and its eigenvalues describe the amount of orientational ordering in each direction.

The bulk free-energy density in the Lanadu–de Gennes theory is written as follows [18,19]:

$$f(\mathbf{Q}) = \frac{1}{2}aQ_{ij}Q_{ij} - \frac{1}{3}bQ_{ij}Q_{jk}Q_{ki} + \frac{1}{4}c(Q_{ij}Q_{ij})^2 + \frac{1}{2}L_1(Q_{ij,k})^2, \tag{1}$$

where summation over repeated indices is implied and the comma indicates spatial derivative with respect to the spatial coordinate x_k. The first three terms describe the nematic-isotropic phase transition. The coefficients are such that $a = \alpha(T - T^*)$, with a, c, and L positive. The temperature T^* is the lowest temperature T, at which the isotropic phase can exist. The presence of cubic term $Q_{ij}Q_{jk}Q_{ki}$ in the homogeneous part implies that the nematic-isotropic phase transition is the first order. For simplicity, one adopts the one-constant form of the elastic energy in the last term.

In this paper, we use the anchoring of the molecules to a bounding surface, which is quantified by Nobili-Durand free-energy density [20]

$$F_s = \frac{W}{2}\int d^2x(Q_{ij} - Q_{ij}^{(0)})^2, \tag{2}$$

where W is the anchoring strength and Q_{ij}^0 is the preferred order parameter at the surface. The surface free energy [Eq. (2)] is compatible with the experimentally measured anchoring in the nematic phase [4,20]. The previous works are based on linear surface energy [9,10] although the best fits of the experimental results are obtained from the quadratic surface energy [4].

The number of parameters is reduced by using a rescaled order parameter $\mu_{ij} = Q_{ij}/s[s = \frac{2\sqrt{6b}}{9c}]$ and temperature $\tau = \frac{27ac}{8b^2}(T - T^*)$. Furthermore, all lengths and the free energy

*erfan.kadivar@pgu.ac.ir

are given, respectively, in units of $\xi=\sqrt{L_1/cs^2}$ and $\Delta f=cs^4$, where $2\sqrt{2}\xi$ denotes the nematic coherence length at the nematic-isotropic phase transition. Introducing also dimensionless surface coupling parameter $\gamma=\frac{W\xi}{L_1}$, which quantifies the competition between surface energy and elastic free energy, the reduced total free energy reads as follows:

$$F=\int d^3x\left(\frac{1}{2}\tau\mu_{ij}\mu_{ij}-\frac{\sqrt{6}}{4}\mu_{ij}\mu_{jk}\mu_{kl}+\frac{1}{4}(\mu_{ij}\mu_{ij})^2+\frac{1}{2}(\mu_{ij,k})^2\right)+\frac{\gamma}{2}\int d^2x(\mu_{ij}-\mu_{ij}^{(0)})^2. \tag{3}$$

Consider a nematic droplet with a reduced radius R_0 which is located at origin. We restrict our attention to case that the director field is radial everywhere. There is only a splay deformation, and according to symmetry of local director, we choose the uniaxial order parameter and uniaxial preferred order parameter as follows:

$$\mu_{ij}=S\left(e_{ri}e_{rj}-\frac{1}{3}\delta_{ij}\right), \tag{4}$$

$$\mu_{ij}^{(0)}=S_0\left(e_{ri}e_{rj}-\frac{1}{3}\delta_{ij}\right), \tag{5}$$

where $\hat{e}_r$ is the unit vector along the redial direction in the spherical coordinate and S is the Maier-Saupe scaler order parameter, which depends on the reduced distance from the center of the particle, r. Thus the reduced total free energy within the spherical droplet reads as follows:

$$\mathcal{F}=\frac{1}{R_0^2}\int_0^{R_0}r^2\left[f_b\pm 6\frac{S^2}{r^2}+\left(\frac{dS}{dr}\right)^2\right]dr+\gamma[S(R_0)-S_0]^2. \tag{6}$$

with the bulk free-energy density

$$f_b=\tau S^2-\frac{1}{\sqrt{6}}S^3+\frac{1}{3}S^4. \tag{7}$$

The upper and lower signs refer to the case that nematic-isotropic phase transition is approached from above and below, respectively. The second term of the integrand in Eq. (6) can be rolled as a shift in temperature. Note that by rescaling the free energy, we are left with four essential parameters: temperature τ, droplet radius R_0, surface anchoring strength γ, and preferred order parameter S_0 that completely determine the wetting behavior of liquid-crystal droplet. According to bulk free-energy density f_b, the bulk nematic-isotropic transition from $S=0$ to $S_b=\frac{\sqrt{6}}{4}$ or vice versa occurs at $\tau_b=0.125$ and $\tau^\dagger=9/64$ is superheating temperature of nematic phase. Variation in the free energy [Eq. (6)] in order to determine the order-parameter profile $S(r)$ that minimizes $\mathcal{F}[S(r)]=\int f(r)d^3\mathbf{r}$ leads to the following differential equation:

$$\frac{d^2S}{dr^2}+\frac{2}{r}\frac{dS}{dr}-\frac{2}{3}S^3+\frac{\sqrt{6}}{4}S^2-\left(\tau\pm\frac{6}{r^2}\right)S=0, \tag{8}$$

together with two boundary conditions at the interface,

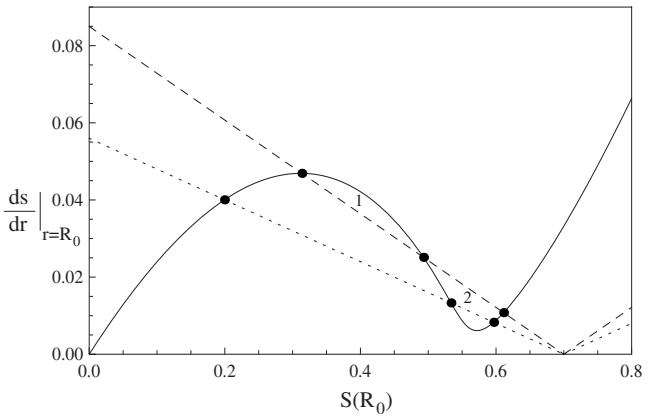

FIG. 1. Graphical solution of Eq. (9) when the nematic-isotropic transition temperature is approached from above. If the areas 1 and 2 are the same, a prewetting transition from the thin film to the thick film solution occurs. The dots are the correct solution of Eq. (9) (see the text for details).

$$\left.\frac{dS}{dr}\right|_{r=R_0}=\gamma[S(R_0)-S_0], \tag{9}$$

and far from surface (at the center of droplet),

$$\left.\frac{dS}{dr}\right|_{r\to 0}=0 \quad \text{or} \quad \lim_{r\to 0}S(r)=S_b, \tag{10}$$

where the orientational order is uniform and where it assumes the bulk value S_b, determined by minimizing the bulk free-energy density f_b of Eq. (7). Differential Eq. (8) is solved numerically by using the relaxation method for arbitrary values of $S(R_0)$. Once order-parameter profile $S(r)$ for each value $S(R_0)$ is obtained, we plot $\frac{dS}{dr}|_{r=R_0}$ as a function of $S(R_0)$. According to Eq. (9), the possible surface order parameters $S(R_0)$ are the intersections with the right side of Eq. (9). Figure 1 illustrates a graphical representation of Eq. (9). The full line and dashed or dotted lines relate to the left and right sides of Eq. (9). When multiple solutions for $S(R_0)$ occur, the correct $S(R_0)$ is that one which gives the absolute minimum value of the total free energy [Eq. (6)]. In the case presented in Fig. 1, three solutions are found. The middle solution always gives a maximum in the free energy. A phase transition between the first and third solutions occurs if areas 1 and 2 are both the same, which is the well-known Maxwell construction (see dashed line in Fig. 1). If area 1 is larger than area 2 (see dotted line in Fig. 1), the first solution gives the absolute minimum of the total free energy or vice versa.

III. RESULT ON APPROACHING THE NEMATIC-ISOTROPIC TRANSITION FROM ABOVE

The critical at bulk phase-transition temperature occurs when the two extremums of $\frac{dS}{dr}|_{r=R_0}$ merge to saddle point. We numerically obtain $R_c=16.6$ [see Fig. 2(b)]. Below the critical radius R_c, the boundary-layer transition between the thin and thick films does not occur inside a liquid-crystal droplet [Fig. 2(c)]. Indeed for $R_0<R_c$ the curves are monotonic functions of $S(R_0)$ [see Fig. 2(c)]. In Fig. 2 the different

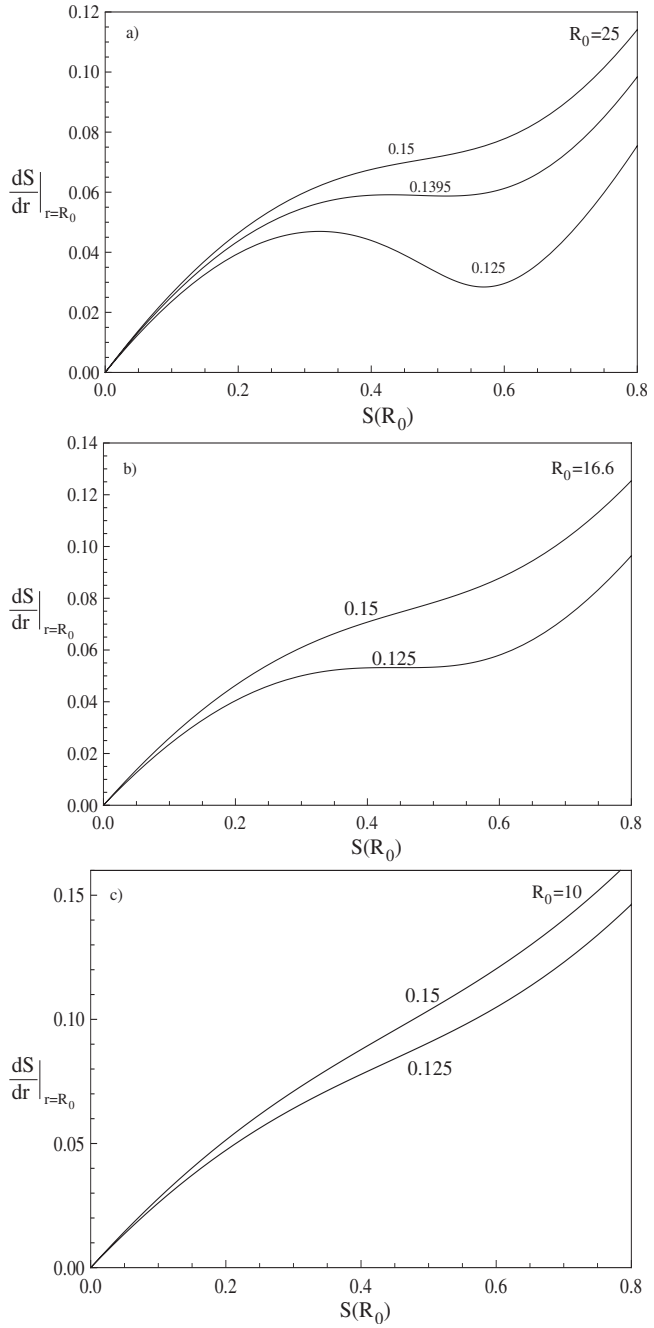

FIG. 2. $\frac{dS}{dr}|_{r=R_0}$ as a function of $S(R_0)$ for different temperatures and different radii: (a) $R_0=25$, (b) $R_0=16.6$, and (c) $R_0=10$ (see the text for details).

curves of each part correspond to different temperatures. Another critical point on temperature, τ_c, for given radius ($R_0 > R_c$) occur when $\frac{dS}{dr}|_{r=R_0}$ as a function of $S(R_0)$ possesses a saddle point [see Fig. 2(a) for $\tau_c=0.1395$]. On basis of such arguments, we plot the critical temperature as a function of droplet radius in Fig. 3. It is noted that in the case of planar surface, the critical temperature is the superheating temperature $\tau^{\dagger}$.

In Fig. 4 the variation in the surface order parameter within an $R_0=35$ droplet at bulk nematic-isotropic temperature as a function of anchoring strength is presented. The

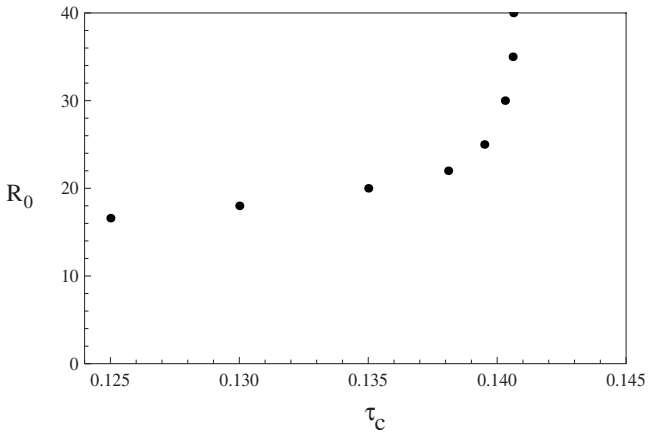

FIG. 3. The critical temperature as a function of droplet radius (see the text for details).

various curves correspond to different values of preferred order parameter of the surface. At $S_0>0.57$, the first-order transitions are manifested by jump in $S(R_0)$. In this case, with increasing the anchoring strength the surface order parameter within a droplet is discontinuity increasing. But it is continuously increasing for $S_0<0.5775$.

In Fig. 5 the change in the surface order parameter within a droplet with as function of anchoring strength is illustrated. The different curves correspond to different temperatures. In the temperature interval $0.125<\tau<0.129$, the droplet is in the paranematic phase at small anchoring strength, but the first-order transition between paranematic to nematic phases occurs as γ increases. At $\tau>0.130$ with increasing anchoring strength the surface order parameter is continuously increasing.

Figure 6 illustrates the relevant wetting phase diagram in the parameter space of the surface potential when the nematic-paranematic phase transition is approached from above. The full line which is determined by the Maxwell construction when areas 1 and 2 in Fig. 6 are equal, separated the regions of complete wetting and partial wetting. The complete wetting corresponds to a thick nematic film which extends close to the surface inside of the droplet when the bulk phase transition is approached with decreasing tem-

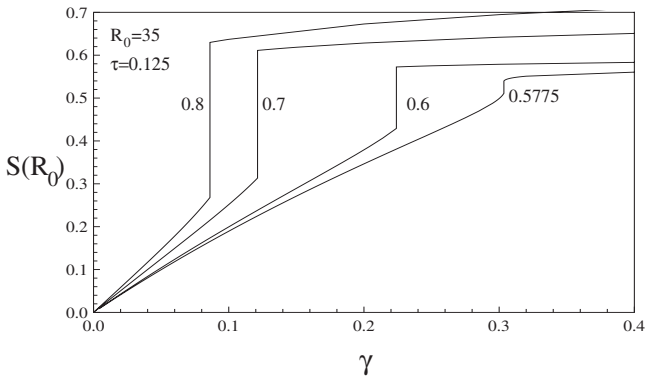

FIG. 4. Calculated order parameter inside of droplet surface with radius $R_0=35$ as function of anchoring for different preferred order parameters at bulk nematic-isotropic transition temperature τ_b (see the text for details).

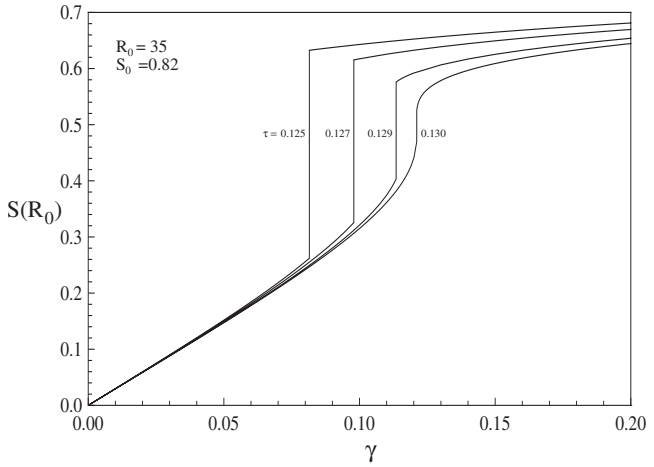

FIG. 5. Calculated order parameter inside of droplet surface with radius $R_0=35$ as function of anchoring for different temperatures (see the text for details).

perature. The length of full line decreases with a decrease in droplet radius until a critical radius R_c that the length of full line completely vanishes. The dashed line is the projection of a critical line on S_0, γ plane at the bulk nematic-isotropic phase-transition temperature. The confined region between the dashed and full line defines the prewetting surface. When crossing this surface with decreasing temperature, the order-parameter profile jumps from the thin film to thick film. With crossing the full line a first-order boundary-layer transition inside of droplet surface occurs. The dashed and full line meet each other in a tricritical point that the coordinate of it in the S_0, γ plane depends on droplet radius. This point is indicated by a filled circle.

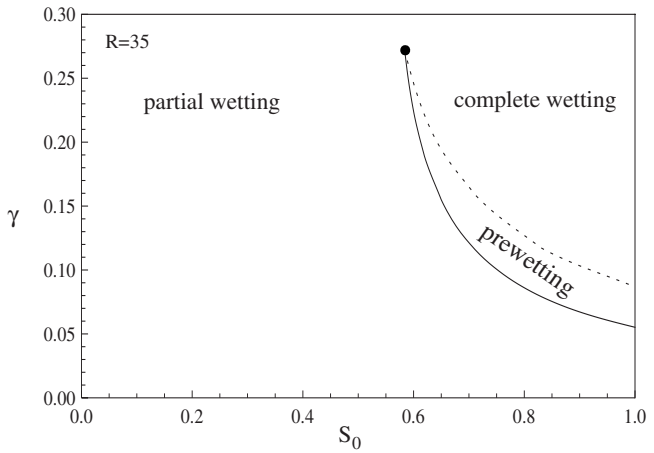

FIG. 6. Wetting phase diagram for nematic wetting when bulk nematic-isotropic transition temperature τ_b is approached from above. The dashed line is the projection of prewetting line on the S_0, γ plane at τ_b. The filled circle indicates a tricritical point for the wetting transitions (see the text for details).

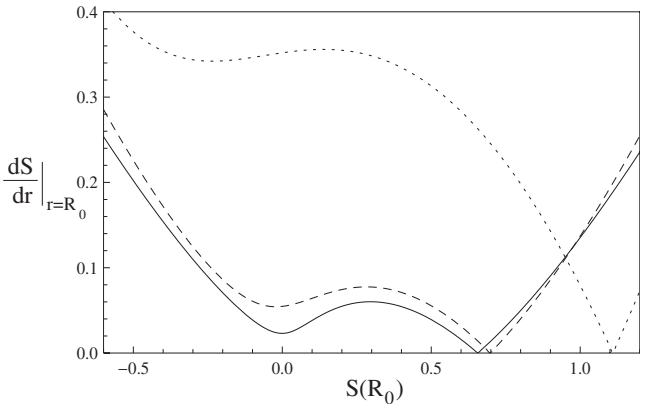

FIG. 7. $\frac{dS}{dr}|_{r=R_0}$ as a function of $S(R_0)$ for different radii when the bulk nematic-isotropic phase-transition temperature is approached below. The full line: $R_0=30$; dashed line: $R_0=20$; and dotted line: $R_0=6$.

IV. DISCUSSION AND CONCLUSIONS

The influence of surface curvature on the prewetting on the nematic wetting behavior inside of droplet has been studied using the Landau–de Gennes theory and quadratic surface energy. We restrict our attention to the strong homeotropic anchoring, i.e., director field is radial everywhere inside of droplet which emerges radially from the central point defect. By using the Maxwell construction, we determine the first-order boundary-layer transition which disappears completely below the critical radius when a bulk nematic-isotropic phase-transition temperature is approached from above. The value of critical radius is about 16.6 in the rescaled frame. Fukuda *et al.* [9] found that there is the critical radius for a solid spherical particle which is dispersed in nematic liquid crystal above bulk nematic-isotropic transition temperature. They reported critical radius about 28.9 in the our scale. By using deuterium NMR measurements, the critical radius in polymer-dispersed liquid crystals (PDLCs) with bipolar droplets was observed by Golemme *et al.* [21]. They reported that the critical diameter of bipolar liquid-crystal droplet is between 0.35 and 0.035 μm.

In the case that bulk nematic-isotropic phase-transition temperature is approached from below by decreasing the droplet radius, the two extremums of $\frac{dS}{dr}|_{r=R_0}$ do not merge to the saddle point, so the boundary-layer transition occurs for each radius (see Fig. 7).

ACKNOWLEDGMENT

The author acknowledges the partial support of Persian Gulf University Research Council.

[1] P. Sheng, Phys. Rev. A **26**, 1610 (1982).
[2] T. J. Sluckin and A. Poniewierski, Phys. Rev. Lett. **55**, 2907 (1985).
[3] J.-B. Fournier and P. Galatola, Europhys. Lett. **72**, 403 (2005).
[4] E. Kadivar, Ch. Bahr, and H. Stark, Phys. Rev. E **75**, 061711 (2007).
[5] E. Kadivar, Phys. Rev. E **78**, 031706 (2008).
[6] R. Holyst and A. Poniewierski, Phys. Rev. B **36**, 5628 (1987).
[7] M. P. Gelfand and R. Lipowsky, Phys. Rev. B **36**, 8725 (1987).
[8] H. Stark, J. Fukuda, and H. Yokoyama, J. Phys.: Condens. Matter **16**, S1911 (2004).
[9] J. I. Fukuda, H. Stark, and H. Yokoyama, Phys. Rev. E **69**, 021714 (2004).
[10] S. Kralj, S. Žumer, and D. W. Allender, Phys. Rev. A **43**, 2943 (1991).
[11] Y. Rosenfeld, Phys. Rev. E **50**, R3318 (1994).
[12] Y. Rosenfeld, Mol. Phys. **86**, 637 (1995).
[13] G. Cinacchi and F. Schmid, J. Phys.: Condens. Matter **14**, 12223 (2002).
[14] P. G. Bolhuis, J. M. Brader, and M. Schmidt, J. Phys.: Condens. Matter **15**, S3421 (2003).
[15] R. Roth, J. M. Brader, and M. Schmidt, Europhys. Lett. **63**, 549 (2003).
[16] J. H. Erdmann, S. Žumer, and J. W. Doane, Phys. Rev. Lett. **64**, 1907 (1990).
[17] P. G. de Gennes and J. Prost, *The Physics of Liquid Crystals*, 2nd ed. (Oxford Science Publications, Oxford, 1993).
[18] E. F. Gramsbergen, L. Longa, and W. H. de Jeu, Phys. Rep. **135**, 195 (1986).
[19] P. G. de Gennes, Mol. Cryst. Liq. Cryst. (Phila. Pa.) **12**, 193 (1971).
[20] M. Nobili and G. Durand, Phys. Rev. A **46**, R6174 (1992).
[21] A. Golemme, S. Žumer, D. W. Allender, and J. W. Doane, Phys. Rev. Lett. **61**, 2937 (1988).